land

MDPI

Article

Land Use Change and Mangrove Restoration Modulate Heavy Metal Accumulation in Tropical Coastal Sediments: A Nearly Decade-Long Study from Hainan, China

Tingting Si [1,2], Penghua Qiu [3,4,*], Lei Li [1], Wenqian Zhou [3], Chuanzhao Chen [5], Qidong Shi [3], Meihuijuan Jiang [3] and Yanli Yang [3]

[1] College of Life Sciences, Hainan Normal University, Haikou 571158, China; sitingting@hainnu.edu.cn (T.S.); lei-li@126.com (L.L.)
[2] College of Tourism, Hainan Normal University, Haikou 571158, China
[3] College of Geography and Environmental Sciences, Hainan Normal University, Haikou 571158, China; 20212070500002@hainnu.edu.cn (W.Z.); 202212070500015@hainnu.edu.cn (Q.S.); jmhj0102@hainnu.edu.cn (M.J.); 920149@hainnu.edu.cn (Y.Y.)
[4] Hainan Provincial Key Laboratory of Ecological Civilization and Integrated Land-Sea Development, Haikou 571158, China
[5] Hainan Guoyuan Institute of Land and Mineral Survey Planning & Design Co., Ltd., Haikou 570203, China; wnccz@163.com
* Correspondence: 110015@hainnu.edu.cn

Abstract: Mangrove forests, vital coastal ecosystems that provide critical biodiversity habitats and carbon sequestration services, face increasing heavy metal pollution that threatens their ecological functions through bioaccumulation and toxicity to marine organisms. However, existing studies lack dynamic insights into temporal and spatial variations of heavy metals in mangrove sediments. This study systematically analyzed two mangrove reserves in Hainan Island, China (Hainan Dongzhaigang National Nature Reserve [DZG] and Hainan Qinglan Provincial Nature Reserve [QL]), by collecting sediment samples in 2014 and 2022, analyzing metals (Cr, Cu, Zn, As, Cd, and Pb) via ICP-MS, and applying the geo-accumulation index, potential ecological risk index, Markov transition matrix, and statistical analyses. Results showed that DZG exhibited rising Cu and Zn levels but declining Cr, As, Cd, and Pb, with Cd showing the most significant decrease (66.83%). In contrast, QL saw only a 42.7% reduction in Cd, while other heavy metals increased. Spatial heterogeneity linked higher concentrations to anthropogenic hotspots, DZG's southeast (industrial/aquaculture inputs), and QL's northwest (urban/industrial discharges). Although ecological risks were generally low, Cd in QL reached a moderate risk level (E_{Cd} = 46.44, $40 \leq E_i < 80$). The large-scale pond-to-mangrove conversion significantly increased vegetation cover, which enhanced sedimentation rates and exerted a "dilution effect" on sediment heavy metals. These findings underscore anthropogenic activities as the dominant driver of heavy metal contamination. We recommend (1) stringent wastewater control near QL, (2) enhanced shipping regulation, and (3) the establishment of mangrove buffers in heavy metal accumulation zones to improve ecological status.

Keywords: mangroves sediment; heavy metals; spatiotemporal variations; ecological risk; land use change

Received: 13 May 2025
Revised: 2 June 2025
Accepted: 9 June 2025
Published: 12 June 2025

Citation: Si, T.; Qiu, P.; Li, L.; Zhou, W.; Chen, C.; Shi, Q.; Jiang, M.; Yang, Y. Land Use Change and Mangrove Restoration Modulate Heavy Metal Accumulation in Tropical Coastal Sediments: A Nearly Decade-Long Study from Hainan, China. *Land* **2025**, *14*, 1259. https://doi.org/10.3390/land14061259

1. Introduction

Mangrove forests are critical ecological zones in tropical and subtropical coastal regions, providing essential services such as wind and wave mitigation, carbon sequestration,

and biodiversity support [1]. Their unique position at the land–sea interface means they face dual pollution threats from terrestrial sources (industrial wastewater, agricultural runoff, and urban sewage) and marine sources (ship discharge) [2]. The dense root systems of mangroves and periodic tidal inundation create conditions that facilitate the accumulation and deposition of heavy metals in mangrove wetlands.

Current research on heavy metals in mangroves primarily focuses on four aspects: (1) the accumulation and distribution of heavy metals [3]; (2) the sources or origins of heavy metals in mangrove sediments [4,5]; (3) the impact of heavy metals, including effects on soil properties, biodiversity, and food chain toxicity, on mangrove ecosystems [6,7]; and (4) the role of mangroves in heavy metal remediation, such as retention by organic matter, redox, and chelation in roots [8]. Despite extensive research on heavy metal content, pollution assessment, and potential risks to mangrove sediments, existing studies have mostly been limited to static analyses at single time points and lack dynamic insights into temporal and spatial variations. These insights are crucial for identifying the sources and routes of heavy metals and for developing and establishing targeted strategies for mangrove restoration and management. For instance, static analyses cannot distinguish whether observed heavy metal concentrations are due to long-term accumulation, recent pollution events, or the effectiveness of restoration efforts. In contrast, a dynamic approach that examines temporal and spatial variations can reveal how metal accumulation patterns respond to both anthropogenic pressures (e.g., land use changes, urbanization, and industrial activities) and restoration interventions. This distinction is essential for understanding the underlying mechanisms driving heavy metal contamination and for evaluating the effectiveness of conservation measures. This temporal dimension is especially crucial in rapidly developing regions like China, where mangrove ecosystems have undergone dramatic transformations.

China's mangrove ecosystems have undergone significant declines since the 1950s, primarily due to large-scale land reclamation and aquaculture development. Between 1973 and 2000 alone, China lost nearly 60% of its mangrove coverage due to anthropogenic pressures [9]. Since 2000, extensive mangrove restoration efforts have been implemented, including the "Southern Mangroves, Northern Tamarisks" wetland restoration project, the "Blue Bay" initiative, and the Mangrove Conservation and Restoration Action Plan (2020–2025), which have changed this trend. Remote sensing data confirm a steady mangrove area recovery from 2001 to 2021 [10]. Empirical studies demonstrate that these active interventions increased regional carbon storage from 2015 to 2021, of which 97% was directly attributable to ecological restoration [11]. Given the national efforts in mangrove restoration and the significant ecological value of Hainan Island's mangroves, this region has become a crucial area for evaluating the effectiveness of these conservation initiatives. Among all regions in China, Hainan Island is of particular significance. Hainan Island is home to China's most diverse and well-preserved mangrove wetlands, with mangrove areas accounting for 33% of the national total. It holds significant conservation value both nationally and globally. Hainan Island hosts 6092.63 ha of mangroves [12], over half of which are concentrated in the Hainan Dongzhaigang National Nature Reserve (DZG) and the Hainan Qinglan Mangrove Provincial Nature Reserve (QL). DZG, the first national mangrove reserve in China and the largest in Hainan, is also one of the initial seven wetland reserves included in the International Important Wetlands List. QL is the second-largest mangrove reserve in Hainan. Unlike DZG, which is a national-level reserve, QL is a provincial-level reserve and is located closer to urban areas, thus experiencing more frequent human impacts. These differences in protection levels and human influence make the two reserves ideal for comparative studies on heavy metal contamination and the effectiveness of mangrove restoration efforts.

To further understand the impacts of these restoration efforts and human activities on mangrove ecosystems, while accounting for natural environmental variability, we posed the following questions: (1) How have the concentrations and spatial distribution of heavy metals, as well as their ecological risks in the mangrove sediments of DZG and QL, changed from 2014 to 2022? (2) What are the primary drivers of these changes, and which factors have been dominant? (3) How have land use changes and mangrove restoration efforts, particularly pond-to-mangrove conversion projects, modulated heavy metal accumulation in these sediments? In this way, we aimed to elucidate the temporal and spatial variations of heavy metal contamination in mangrove sediments, identify the key factors influencing these changes, and assess the effectiveness of mangrove restoration efforts. Ultimately, we expect to provide robust scientific evidence for the protection of mangrove ecosystems and the evaluation of restoration initiatives, contributing to the sustainable management and conservation of these invaluable coastal habitats.

2. Materials and Methods

2.1. Study Area

DZG is China's oldest mangrove reserve, established in 1980. DZG is located in the northeastern part of Haikou City (Figure 1) and spans 110°32′0″ E—110°38′6″ E, 19°52′30″ N—21°1′0″ N, covering 3337.6 ha, of which 1771.08 ha is mangrove area. The reserve includes two towns (Yanfeng and Sanjiang), with an average annual temperature of 23.8 °C and precipitation of 1670 mm. The reserve hosts 36 species of true and semi-mangrove plants.

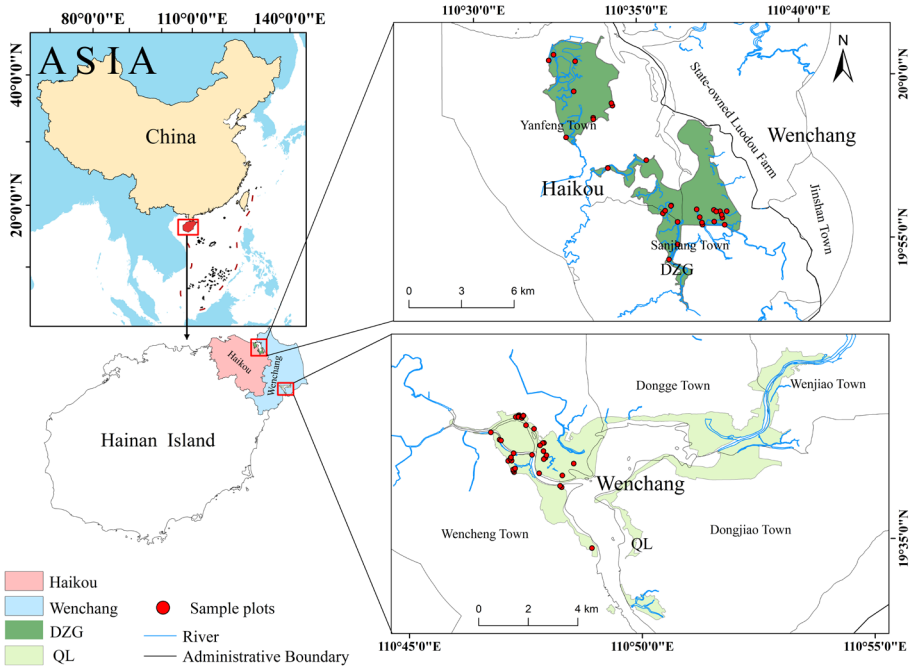

Figure 1. Location of the study area and distribution of sampling sites.

QL was established in 1981 and is located in the central-eastern part of Wenchang City. It spans 110°45′50″ E—110°54′10″ E, 19°33′10″ N—19°39′10″ N and consists of three sections, with the largest (2155.84 ha) being the Bamen Bay section, which includes 781.93 ha of mangrove area. The reserve covers five towns (Wencheng, Dongjiao, Wenchang, Dongge, and Longlou), with an average annual temperature of 24.1 °C and precipitation of 1749 mm. This reserve hosts 44 species of true and semi-mangrove plants.

These distinct geographical settings, climatic conditions, and anthropogenic pressures between DZG and QL are expected to differentially influence heavy metal accumulation

patterns, providing an ideal comparative framework to assess how natural and human factors modulate sediment metal dynamics in mangrove ecosystems.

2.2. Field Sampling and Laboratory Analysis

In July 2014 and July 2022, 61 sample plots (including 28 in DZG and 33 in QL) were established in the two nature reserves. In each plot, three 10 m × 10 m quadrants were randomly established to act as representative mangrove species. Sediment samples (0–20 cm depth) were collected using a real-time kinematic global positioning system (RTK-GPS) for accurate positioning. After air-drying in the laboratory, samples were cleaned, ground, sieved, and stored for later analyses. Heavy metals (Cr, Cu, Zn, As, Cd, Pb) were analyzed using Agilent 7700× ICP-MS (Agilent, Santa Clara, CA, USA). Organic carbon (OC) and organic matter (OM) were determined by potassium dichromate oxidation spectrophotometry using V-1200 Visible Spectrophotometer (INESA Analytical Instrument Co., Ltd., Shanghai, China). Total nitrogen (TN) was measured by Kjeldahl method with BSA224S Electronic Balance (Sartorius AG, Göttingen, Germany). Total phosphorus (TP) was analyzed via alkali fusion-molybdenum antimonate spectrophotometry (V-1200 Spectrophotometer), and total potassium (TK) by atomic absorption spectrometry (AA-7000 spectrometer, Shimadzu Corp., Kyoto, Japan).

Additionally, the land use/cover datasets for the years 2015 and 2023 were obtained from the official Land Use Change Monitoring Survey database maintained by China's Land Resources Department.

2.3. Methods

2.3.1. Geo-Accumulation Index (I_{geo})

The geological accumulation index (I_{geo}), also known as the Muller index, considers both natural geological background values and anthropogenic effects on heavy metal pollution [13] and is calculated using Formula (1):

$$I_{\text{geo}} = \log_2\left[C_S^{\text{i}}/(K \times C_n^{\text{i}})\right] \quad (1)$$

in which I_{geo} is the geological accumulation index, C_S^{i} is the measured concentration of heavy metal i (mg/kg), C_n^{i} is the geochemical background value of heavy metal i (mg/kg) based on the chemical element abundance of China's shallow marine sediments [14], and 1.5 is a correction factor for possible variations in background values. The classification criteria included $I_{geo} \leq 0$ (unpolluted), $0 < I_{geo} \leq 1$ (lightly–moderately polluted), $1 < I_{geo} \leq 2$ (moderately polluted), $2 < I_{geo} \leq 3$ (moderately–strongly polluted), $3 < I_{geo} \leq 4$ (strongly polluted), $4 < I_{geo} \leq 5$ (very strongly polluted), and $I_{geo} > 5$ (extremely polluted).

2.3.2. Potential Ecological Risk Index (RI)

The potential ecological risk index (RI), proposed by Hakanson [15] is widely used for pollution and ecological risk assessments. This index incorporates both heavy metal concentrations in addition to their toxicity and mobility [16]. It is calculated using the formula shown below:

$$RI = \sum E_i = \sum T_i \times \frac{C_i}{P_i} \quad (2)$$

in which E_i is the potential ecological risk of heavy metal i, T_i is the toxicity coefficient (Zn = 1, Pb = Cu = 5, Cd = 30, As = 10, Cr = 2; [17]), C_i is the measured concentration, and P_i is the reference value based on the first-class standards of the "Technical Specifications for the Assessment of Seawater, Marine Sediment, and Marine Biological Quality" [18]. The ecological risk is classified as shown: $E_i < 40$ (low), $40 \leq E_i < 80$ (moderate), $80 \leq E_i < 160$ (high), $160 \leq E_i < 320$ (very high), $E_i \geq 320$ (extremely high); RI < 150

(low), $150 \leq RI < 300$ (moderate), $300 \leq RI < 600$ (high), $600 \leq RI < 1200$ (very high), and $RI \geq 1200$ (extremely high).

2.3.3. Markov Transition Matrix (MTF)

The Markov transition matrix describes the probability of transitions between system states and is suitable for analyzing spatiotemporal changes in land use types. Land use is a key factor in global environmental change and a direct reflection of human activities on the natural environment [19]. This study uses the Markov transition matrix to describe the spatiotemporal characteristics and transition directions of mangrove land use types.

2.3.4. Statistical Analysis

A Pearson's correlation analysis was used to assess the relationships between heavy metal concentrations and sediment physicochemical properties to reveal potential associations. A principal component analysis (PCA) identified key environmental factors influencing heavy metal distribution and supported the identification of potential sources. A redundancy analysis (RDA) was used to further explore the main associations between heavy metals and environmental factors, visually present the dynamic characteristics of heavy metal distribution, and provide insights into how environmental factors interact to shape the spatial distributions of heavy metals in sediments.

3. Results

3.1. Temporal and Spatial Variations of Heavy Metals in Mangrove Sediments

3.1.1. Temporal Variations

Figure 2 shows that in the DZG, the concentrations of Cu and Zn in mangrove sediments increased from 2014 to 2022, while Cr, As, Cd, and Pb decreased. Specifically, Cd, Pb, As, and Cr decreased by 66.83%, 40.31%, 26.56%, and 22.36%, respectively. The element concentration order in DZG sediments changed from Zn > Cr > Pb > As > Cd > Cu in 2014 to Zn > Cr > Pb > Cu > As > Cd in 2022. In QL, the Cd concentration decreased by 42.7%, while Cr, Cu, Zn, As, and Pb concentrations increased. The element concentration order in QL sediments changed from Zn > Cr > Pb > As > Cu > Cd in 2014 to Zn > Cr > Cu > Pb > As > Cd in 2022.

Overall, the Cd concentrations in both reserves decreased significantly, and most heavy metals remained at low levels. According to the "Technical Specifications for the Assessment of Seawater, Marine Sediment, and Marine Biological Quality" (HJ1300-2023), all six heavy metals in DZG sediments were at the "excellent" level in 2022, except for Cr, which was at the "medium" level in 2014. In QL, Cr was at the "medium" level in 2022, while other metals were at the "excellent" level.

3.1.2. Spatial Variations

Using the chemical element abundance of China's shallow marine sediments and marine sediment quality evaluation standards, we mapped the spatial distribution of heavy metals using inverse distance weighting interpolation. The results were categorized into three classes: (1) near-natural background values (below the chemical element abundance, as shown in blue); (2) meeting China's Class I standards (between the chemical element abundance and "excellent" level, as shown in yellow); and (3) meeting China's Class II standards (within the "medium" range, as shown in red).

Figure 3(A1,A2) show that in DZG, Cr decreased in the northwest and southeast but increased in the central-southern region (reaching the "medium" level) in 2022. In QL, Cr increased across most areas (reaching the "medium" level) except for a slight decrease in the mid-western region (Figure 3(A3,A4)). The Cu concentrations in DZG remained at

near-natural background values, with no significant changes (Figure 3(B1,B2)), while in QL, Cu increased in the northwest and northeast in 2022 (Figure 3(B3,B4)).

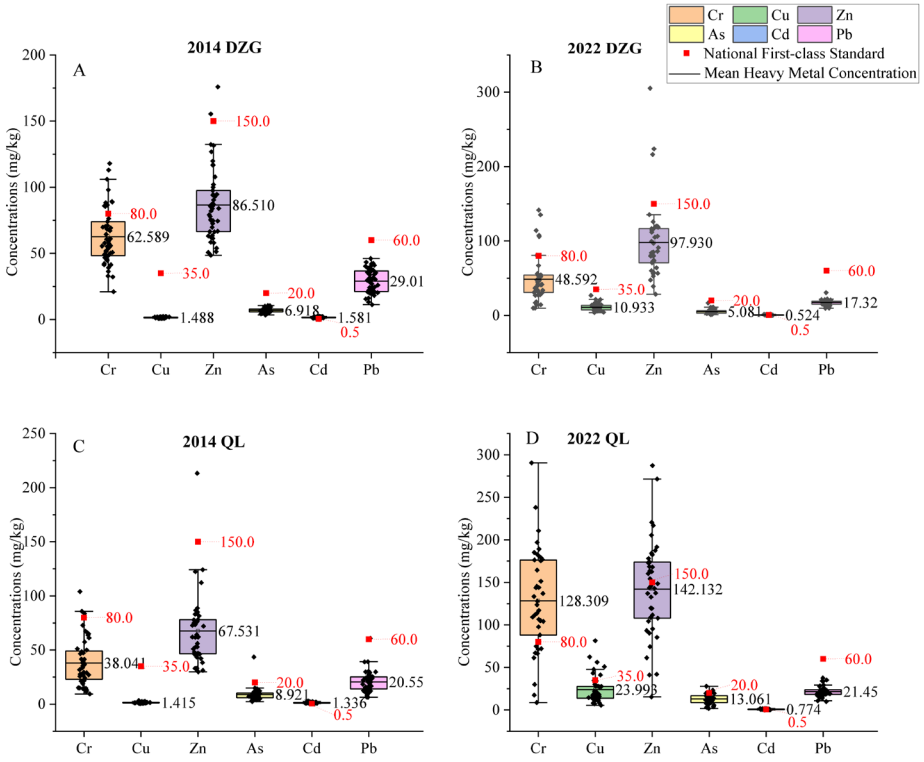

Figure 2. Heavy metal concentrations from mangrove sediments from study areas in different years. (**A**) shows DZG in 2014. (**B**) shows DZG in 2022. (**C**) shows QL in 2014. (**D**) shows QL in 2022.

In DZG, the Zn concentrations increased in the northwest and south of Yanfeng Town (reaching the "medium" level) but decreased in other areas (remaining at the "excellent" level) in 2022 (Figure 3(C1,C2)). In QL, the Zn concentrations rose across most areas, especially in the northwest of Wencheng Town (reaching the "medium" level), while other regions remained at the "excellent" level (Figure 3(C3,C4)). The concentrations in DZG improved overall and approached natural background levels (Figure 3(D1,D2)), while in QL, As increased in most areas except for a slight decrease in the northwest of Wencheng Town (Figure 3(D3,D4)).

Overall, the Cd concentrations in the DZG decreased with the exception of the "medium" level in Sanjiang Town (Figure 3(E1,E2)). In QL, Cd decreased in most areas but remained at the "medium" level in parts of Wencheng and Wenchang and Dongge Towns (Figure 3(E3,E4)). The Pb concentrations in both reserves remained at the "excellent" level with a noticeable decrease from 2014 to 2022. In DZG, nearly all areas had reached near-natural background concentrations, with only a minor southern section near Sanjiang Town remaining at the National Grade I threshold (Figure 3(F1,F2)). Similarly, QL demonstrated widespread improvement across most zones, with concentrations approaching natural levels, except for its northwestern part of Wencheng Town, where the Pb levels remained at the National Grade I level without significant reduction (Figure 3(F3,F4)).

In summary, spatial heterogeneity of heavy metals was evident in both reserves. In the DZG, concentrations were lower in the northwest than in the southeast, while in QL, concentrations were lower in the south than in other regions. Compared to 2014, the Cr and Cd in DZG decreased significantly in the western region, but the Cd in the southeast still exceeded China's Class I standard. In QL, the Cr and Cd exceeded China's Class I standard, and Cu, Zn, and As exceeded Class I standards in the northwest with the largest areas exceeding the standard for Zn > Cu > As.

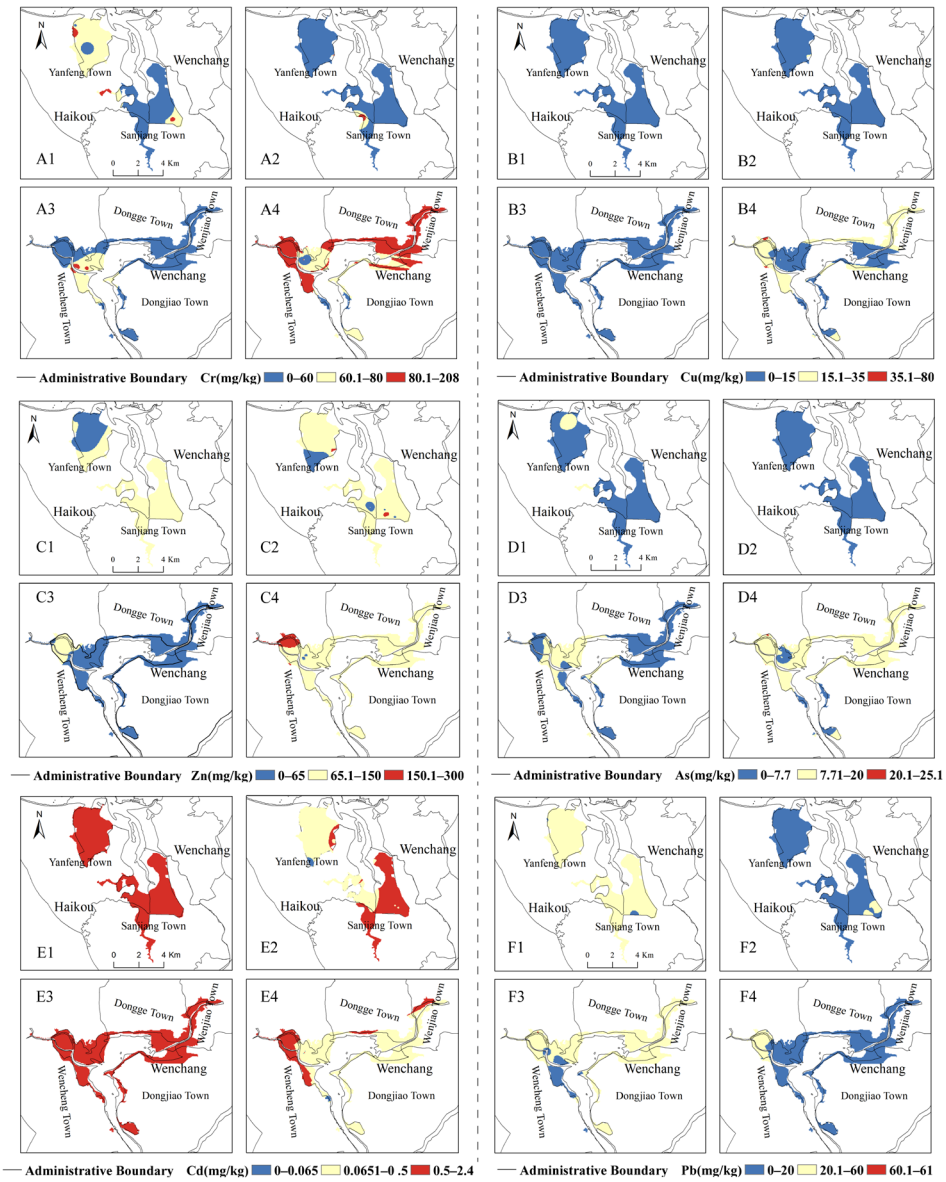

Figure 3. Heavy metal distribution in mangrove sediments at DZG and QL (2014–2022). (**A1**,**A2**) show Cr in DZG in 2014 and 2022. (**A3**,**A4**) show Cr in QL in 2014 and 2022. (**B1**,**B2**) show Cu in DZG in 2014 and 2022. (**B3**,**B4**) show Cu in QL in 2014 and 2022. (**C1**,**C2**) show Zn in DZG in 2014 and 2022. (**C3**,**C4**) show Zn in QL in 2014 and 2022. (**D1**,**D2**) show As in DZG in 2014 and 2022. (**D3**,**D4**) show As in QL in 2014 and 2022. (**E1**,**E2**) show Cd in DZG in 2014 and 2022. (**E3**,**E4**) show Cd in QL in 2014 and 2022. (**F1**,**F2**) show Pb in DZG in 2014 and 2022. (**F3**,**F4**) show Pb in QL in 2014 and 2022.

3.2. Potential Ecological Risk Assessment of Heavy Metals in Mangrove Sediments

3.2.1. Analysis of Geo-Accumulation Index Differences

Table 1 shows that in the DZG, Cd was at extreme pollution levels in 2014, while Cr, Cu, Zn, As, and Pb were at unpolluted levels. By 2022, Cd pollution decreased to moderate–high levels, and Zn shifted to light–moderate pollution. In QL, Cr, Cu, Zn, As, and Pb were unpolluted in 2014, while Cd was at high pollution levels. By 2022, Pb remained unpolluted, but Cr, Cu, Zn, and As shifted to light–moderate pollution levels, and Cd decreased to moderate–high levels.

Table 1. Analysis of geo-accumulation index and potential ecological risk index in the study areas across different years.

Study Area	Year	$I_{geo\ Cr}$	$I_{geo\ Cu}$	$I_{geo\ Zn}$	$I_{geo\ As}$	$I_{geo\ Cd}$	$I_{geo\ Pb}$	E_{Cr}	E_{Cu}	E_{Zn}	E_{As}	E_{Cd}	E_{Pb}	RI
DZG	2014	−0.548	−3.919	−0.173	−0.739	4.019	−0.048	1.56	0.64	0.58	3.46	94.86	7.25	108.35
	2022	−0.913	−1.041	0.006	−1.185	2.427	−0.792	1.21	4.69	0.65	2.54	31.57	3.33	43.99
QL	2014	−1.266	−3.991	−0.53	−0.366	3.776	−0.546	0.95	0.61	0.45	4.46	80.16	1.71	88.34
	2022	0.488	0.093	0.544	0.177	2.991	−0.484	3.21	10.28	0.95	6.53	46.44	1.79	69.2

Figure A1 shows that the Cd pollution in both the DZG and QL areas was significantly higher than that due to other heavy metals across different years. In the DZG, Cd pollution at high or above levels decreased from 97.87% in 2014 to 23.08% in 2022, with a 74.8% reduction. Pb pollution decreased significantly, with 97.44% of samples at unpolluted levels in 2022. In QL, Cd pollution decreased from 90.91% at high or above levels in 2014 to 53.66% in 2022, while Cr, Cu, Zn, and As pollution increased.

The I_{geo} indicates that although the Cd levels in the DZG and QL have undergone a decrease over the past decade, they still remain relatively high. In contrast, the Cr, Cu, Zn, and As levels in QL increased.

3.2.2. Potential Ecological Risk Index Analysis

The potential ecological risk assessment results for mangrove sediments in the study areas are shown in Table 1. In DZG, the values of Cr, As, Cd, and Pb decreased from 2014 to 2022, while Cu and Zn increased. Overall, except for Cd, which posed a high risk in 2014, the other five heavy metals were at low risk levels in both years. By 2022, the risk level of Cd decreased to a low level. The overall ecological RI in the DZG significantly decreased from 108.35 in 2014 to 43.99 in 2022 and then remained at a low risk level. In QL, the value of Cd decreased from a high to a moderate risk, while Cr, Cu, Zn, As, and Pb increased but remained at low risk levels. The RI in QL decreased from 88.34 in 2014 to 69.20 in 2022 and then remained at a low risk level. Thus, both DZG and QL exhibited low overall ecological risks, but the Cd levels, especially in QL, warrant attention.

4. Discussion

4.1. Comparison of Heavy Metal Content in Mangrove Sediments with Other Regions

When compared with other domestic and international regions (Table 2), the heavy metal content in the study area was found to generally have moderate-to-low pollution levels, with significant temporal and spatial differences. Specifically, the Cr content in QL in 2022 (128.31 mg/kg) was significantly higher than that in DZG (48.59 mg/kg) and Shenzhen Futian, China (55.4 mg/kg), and close to that in the Pichavaram mangroves in India (141.2 mg/kg), thus reflecting the cumulative effect of intensified industrial activities in QL. The Cu and Zn contents in DZG and QL in 2022 (10.93/97.93 mg/kg and 23.99/142.13 mg/kg, respectively) were lower than those in the industrially intensive Nansha, Guangdong (Cu: 113 mg/kg), and Shenzhen Futian (Zn: 296.3 mg/kg) but significantly higher than those in Queensland, Australia (Cu: 3.1–30.2 mg/kg). Such results highlight the gradient differences in human activities across regions. The As and Cd (13.06 and 0.77 mg/kg, respectively) contents in QL were comparable to those in the mangroves of Bangkok, Thailand (As: 11.91–25.74 mg/kg; Cd: 0.035–0.07 mg/kg), but lower than those in Pichavaram, India (Cd: 11.2 mg/kg), indicating that tropical regions may generally face the risk of As-Cd co-pollution. Overall, the study area has a lower pollution level than the industrialized coastal zones, but variations in content and potential ecological risks across different regions and times within the area still require attention.

Table 2. Comparison of heavy metals in sediments between the study area and other regions (mg/kg).

Study Area	Sampling Time	Cr	Cu	Zn	As	Cd	Pb	References
DZG	2014	62.59	1.49	86.51	6.92	1.58	29.02	This study
	2022	48.59	10.93	97.93	5.08	0.52	17.32	This study
QL	2014	38.04	1.42	67.53	8.92	1.34	20.55	This study
	2022	128.31	23.99	142.13	13.06	0.77	21.46	This study
Futian, Shenzhen, China	2014	55.4	31.7	296.3	- [1]	2.3	47.8	[20]
Nansha, Guangdong, China	2012	155	113	159	-	0.8	55.3	[21]
Maowei Sea, Guangxi, China	2012	30.02	24.81	59.85	11.56	0.34	18.31	[22]
Shankou, Guangxi, China	2016	61.88	14.95	56.44	7.67	0.11	25.97	[23]
Southeastern Queensland, Australia	-	13.3–54.3	3.1–30.2	40.8–144	13	0.1–1.9	20.1–80.9	[24]
Pichavaram, India	2015	141.2	43.4	93	-	11.2	6.6	[25]
Southeast Coast, India	1995	194.83	506.2	126.8	-	6.58	32.36	[26]
Gulf of Mannar, India	-	177	57	73	5.1	0.16	16	[27]
Samut Sakhon Mangrove, Bangkok, Thailand	2009	-	7.90–21.19	55.99–75.05	-	0.035–0.07	11.91–25.74	[5]
Northwest Coast of South America	-	94.3	253.8	678.3	12.2	1.9	81.3	[28]

[1] "-" Indicates missing data.

4.2. Analysis of the Causes of Spatiotemporal Variations in Heavy Metal Content in Mangrove Sediments

4.2.1. Analysis of Heavy Metal Sources

Temporal and spatial variations in heavy metal content in sediments are closely related to their inputs and outputs. A correlation analysis (Figure A2) indicates that in DZG in 2014, Cu strongly correlated with Zn and Pb ($p < 0.001$), while in 2022, all six heavy metals exhibited strong positive correlations, indicating higher similarities between metals or common sources of heavy metals in 2022 compared to 2014. In QL, Cr showed a positive correlation with Cu, As, Cd, and Pb in 2022, whereas Zn shifted from positive to no correlation with Cu and Pb. The negative correlation between As and Cd in 2014 turned positive in 2022, suggesting a shift from different to common sources. These changes indicate increasing complexity in heavy metal sources in QL.

Heavy metals in mangrove sediments originate from both natural factors, such as surface runoff, atmospheric deposition, and rock weathering, as well as anthropogenic activities, such as industrial and agricultural activities and urban development [29]. According to Hainan's ecological environment report, atmospheric deposition can be neglected because the air quality was high (98.63% of days with good air quality) from 2014 to 2022.

(1) Surface Runoff Analysis

The main water systems around the DZG include the Yanfeng West River (40.15 km^2, 20.3 km), Yanfeng East River (76.97 km^2, 31.5 km), Sanjiang Creek (85.60 km^2, 25.01 km) and Yanzhou River (287.67 km^2, 50 km) in Haikou, and the Zhuxi River (386.17 km^2, 46.2 km) in Wenchang. QL is surrounded by the Wenchang and Wenjiao Rivers (403.76 km^2, 37 km and 523.95 km^2, 57 km, respectively). Compared to 2014, the main changes in land use types in the catchment areas by 2022 can be represented by several concomitant changes: (1) In the DZG, increases in forest land, facility agricultural land, urban land, industrial and mining land, and transportation land occurred, and decreases in arable land and orchard land were noted and (2) in QL; increases in orchard land, forest land, aquaculture ponds, facility agricultural land, urban land, industrial and mining lands, and transportation land were found; and a significant decrease in arable land was detected (Table A1). The increase in human-related land use types (orchard land, aquaculture ponds, facility agricultural land, industrial and mining land, and transportation land) was more pronounced in QL

than in DZG, indicating stronger anthropogenic disturbances had occurred in QL. The data suggest that agricultural structural adjustments in DZG may have led to a reduction in agricultural non-point source pollution from surface runoff, while QL showed the opposite trend. Additionally, urbanization, industrialization, and transportation development in QL likely contributed to heavy metal pollution more than in DZG.

(2) Analysis of Rock Weathering Impacts

The vicinity and bottom of Dongzhaigang are predominantly composed of Quaternary volcanic rocks (basalt), whereas Qinglangang primarily features Permian to Triassic and Middle Jurassic granites. Previous studies have indicated that the Cd concentrations in basalt are over twice those in granite [30], with significantly higher As levels in basalt compared to granite. This geological difference results in higher Cd levels in DZG compared to QL, as basalt releases more Cd through weathering processes than granite [31]. These lithological differences would naturally produce higher background Cd concentrations in DZG through enhanced weathering release, as evidenced by the 2014 measurements (DZG: 1.58 mg/kg > QL: 1.34 mg/kg). However, the reversal of this pattern by 2022 (QL: 0.77 mg/kg > DZG: 0.52 mg/kg) suggests that anthropogenic influences have superseded the underlying geochemical controls in recent years.

(3) Analysis of the Impact of Industrial and Agricultural Activities

Human activities, including industrial wastewater discharge, urban sewage, mechanical wear, and ship lubricant leakage [32], are significant sources of Pb. Cr and Cu mainly originate from industrial processes, such as electronics, plating, textiles, and leather tanning [33], while Cr is also linked to agricultural sewage sludge use [34]. Zn and Cu contents have been positively correlated with shrimp farming [35], agricultural activities [36], and shipping [37]. Cu and Zn contents have been significantly and positively correlated with population size [38]. They are mainly produced from wood preservatives and pesticides [39], industrial and aquaculture wastewater, and are associated with shipping traffic, which may also contribute to As deposition. The higher Zn content in the DZG and QL may be related to the development of shrimp farming [34]. Shrimp ponds require artificial feed, but due to low utilization rates, large amounts of organic waste and heavy metals are discharged into surrounding mangrove areas and coastal waters via aquaculture effluents. Studies by Cao et al. [40] indicate that aquaculture ponds are the primary sources of pollution that are associated with DZG's water quality.

Land use changes around the protected areas can indirectly reflect the impact of human activities. From 2015 to 2023, within a 5 km radius of DZG (Figure 4A), the three land use types with the largest inflow areas were other water areas and water conservancy land, mangrove, and non-mangrove forest land with areas of 600, 319, and 186 ha, respectively. The increase in mangrove land was found to have come mainly from pond-to-mangrove conversion, with 222 ha of aquaculture ponds undergoing conversion to mangrove land, which accounted for 64% of the mangrove inflow area. During the same period, industrial and mining land and transportation land had net inflows of 38 and 46 ha, respectively, which may have led to an increase in the Cu and Zn contents in mangrove sediments. The largest outflow area was arable land (645 ha) followed by aquaculture ponds (371 ha) and orchard land (157 ha), as shown in Figure 4A.

From 2015 to 2023, within a 5 km radius of QL (Figure 4B), the top-three land use types with the largest inflow areas were orchard land, non-mangrove forest land, and transportation land, with net inflows of 1729, 1549, and 395 ha, respectively. The increase in orchard and non-mangrove forest land mainly came from urban and residential land in addition to arable land. Mangrove land increased by 154 ha and mainly originated from non-mangrove forest land and aquaculture ponds. This land accounted for 60.68% and

29.91% of the mangrove inflow area, respectively. Industrial and mining lands expanded with a net inflow of 148 ha. Tire friction from transportation and ship wastewater have been recognized as significant sources of heavy metal pollution. Over the past decade, QL has seen increases in Cr (notable), Cu, Zn, As, and Pb contents, except for Cd. This change may be related to the severe impact of urban sewage, industrial wastewater, and aquaculture effluents on the area [41]. The Central Third Ecological Environment Protection Inspection Team noted that QL's seawater quality deteriorated from Class II in 2020 to Class IV or below in 2022, which is a finding that indirectly confirms the previous speculation.

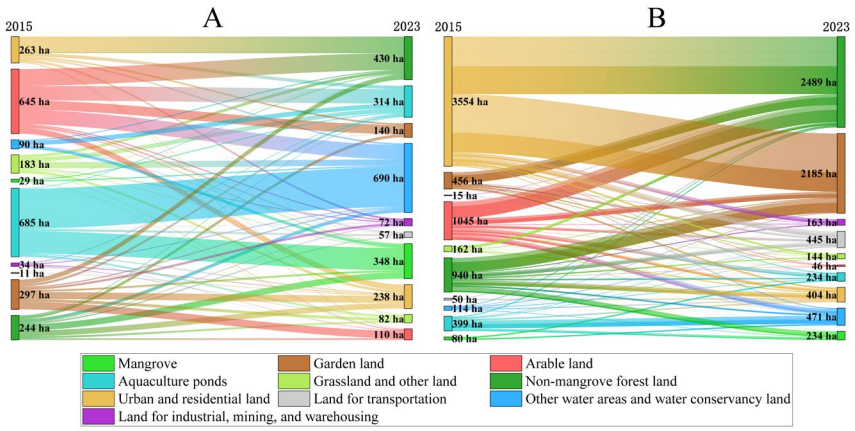

Figure 4. Sankey diagram of land use transition within 5 km radius of the study area. (**A**) shows DZG from 2015 to 2023. (**B**) shows QL from 2015 to 2023.

The spatial distribution of heavy metals in mangrove ecosystems is influenced by multiple factors, with sediment movement and storage being the core processes [42]. Although the northwest part of DZG has a higher population density, the southeast part has more concentrated industrial and mining activities and aquaculture in addition to ship docking terminals. This type of distribution may explain why the northwest and central parts of DZG have relatively lower heavy metal contents, while the southeast part has higher levels. In QL, the south has relatively lower heavy metal contents, while the northwest and northeast have higher levels. Except for the central part in which the Cd and Pb contents decreased, other elements increased to varying degrees in the west, central, and eastern parts. The Cr and Cd contents exceeded China's Class I standards, and in the northwest, the Cu, Zn, and As contents exceeded China's Class I standards. The northwest and northeast are located at the mouths of the Wenchang and Wenjiao Rivers, respectively. Heavy metals carried by rivers gradually deposit during the estuarine process, which is a process that leads to higher heavy metal contents in these areas. Additionally, the northwest part is closer to the city center and surrounded by industrial enterprises, which is another important reason for the higher heavy metal content. Compared to 2014, other heavy metal contents in the western part of DZG, except for Zn, have declined and now reflect the positive effects of the pond-to-mangrove ecological restoration project.

To explore the heavy metal elements and their driving factors in the study area's sediments, indicators such as Cr, Cu, Zn, As, Cd, Pb, OC, OM, TN, TP, and TK were selected for analysis. Additionally, spatial distances to different land use types were calculated to assess their potential influence on heavy metal distribution. Specifically, we employed Near Analysis (ArcGIS 10.8.1) to compute Euclidean distances from each sediment sample to the nearest industrial and mining enterprises (GK_DIST), residential areas (JM_DIST), aquaculture ponds (YZ_DIST), arable land (GD_DIST), and orchard land (YD_DIST). These distances were then included in the correlation analysis, PCA, and redundancy analysis to identify the key factors driving heavy metal variations. The CA (Figure 5A,B) shows a

comparison of heavy metals correlations in 2014 and 2022 in which heavy metal correlations in DZG strengthened in 2022, while correlations with environmental factors weakened, a finding that indicates a shift in heavy metal sources to more homogeneity and reduced human impact. In 2014, Cu, Zn, and Cd showed strong positive correlations, indicating similar sources. These metals were positively correlated with TP and negatively correlated with distance to industrial and mining enterprises, a finding that indicates that higher metal contents were found closer to these enterprises. Zn had strong correlations with many environmental factors. It showed a significant positive correlation with TP and strong positive correlations with OC and OM. It was also negatively correlated with distances to industrial and mining enterprises, aquaculture ponds, arable land, and orchard land, indicating that human activities (industrial and mining activities, planting, and aquaculture) strongly interfered with the heavy metal contents in DZG. In 2022, Cu, Zn, and Cd were not correlated with TP or distance to industrial and mining enterprises. Zn maintained positive correlations with OC and OM but lost any correlations with other previously related environmental factors. This finding shows that with environmental improvements, human activities' impact on mangrove sediment heavy metal contents has decreased.

Compared to 2014, the heavy metal correlations in QL in 2022 were more complex than in DZG (Figure 5C,D). Cu became positively correlated with As, Cd, and Pb, and Cr shifted from negative to positive or to no correlation with other heavy metals. Correlations between heavy metals and environmental factors also changed significantly during this period. For example, As and Cd became positively correlated with OC and TP, and Pb became positively correlated with OC. Cu, Zn, and Cd lost the correlations with distance to orchard land, and As lost the correlation with TN. Cr shifted from a positive to negative correlation in terms of distance to arable land, and Cr, Cu, and Cd became negatively correlated with distance to industrial and mining enterprises.

The PCA (Figure 5E) indicates that in the DZG, OC, OM, and distance to industrial and mining enterprises were the main factors influencing the Cd and Pb contents in 2014, while aquaculture and orchard planting were the main factors influencing Cu and Zn contents in 2022. Heavy metals in QL mangrove sediments are influenced by multiple environmental factors, with key factors including organic matter content, nutrient input, and spatial distribution of human activities. In 2014, Pb, TP, and TN showed strong positive correlations with the first principal component (Figure 5F). Pb is usually related to traffic emissions, while TP and TN are most likely related to agricultural activities and sewage discharge, indicating their association with organic matter content and nutrient input. Cr, Cu, As, and Zn showed positive correlations with the second principal component, suggesting similar sources or involvement of environmental processes in the production of QL's sediments. From 2014 to 2022, the heavy metal contents in QL increased significantly in terms of Cr and Cu, a finding most likely due to increased industrial and agricultural activities and rapid urbanization in the area.

The redundancy analysis (Figure 5G) indicates that in DZG, RDA1 explained 68.45% of the variation, and RDA2 explained 15.61% of the variation. The data points in 2022 were mostly negative on the RDA1 axis, while those in 2014 were more widely distributed on the RDA2 axis. Given that the direction and length of axes reflect environmental gradients, and points on axes represent sample distribution along these gradients, it can be inferred that GK_DIST and JM_DIST had a significant impact on heavy metal distribution in DZG mangroves in 2014. In 2022, TN and YZ_DIST had a greater impact on sediment heavy metal distribution than GK_DIST and JM_DIST, suggesting that aquaculture ponds and industrial and mining enterprises significantly influenced species distribution.

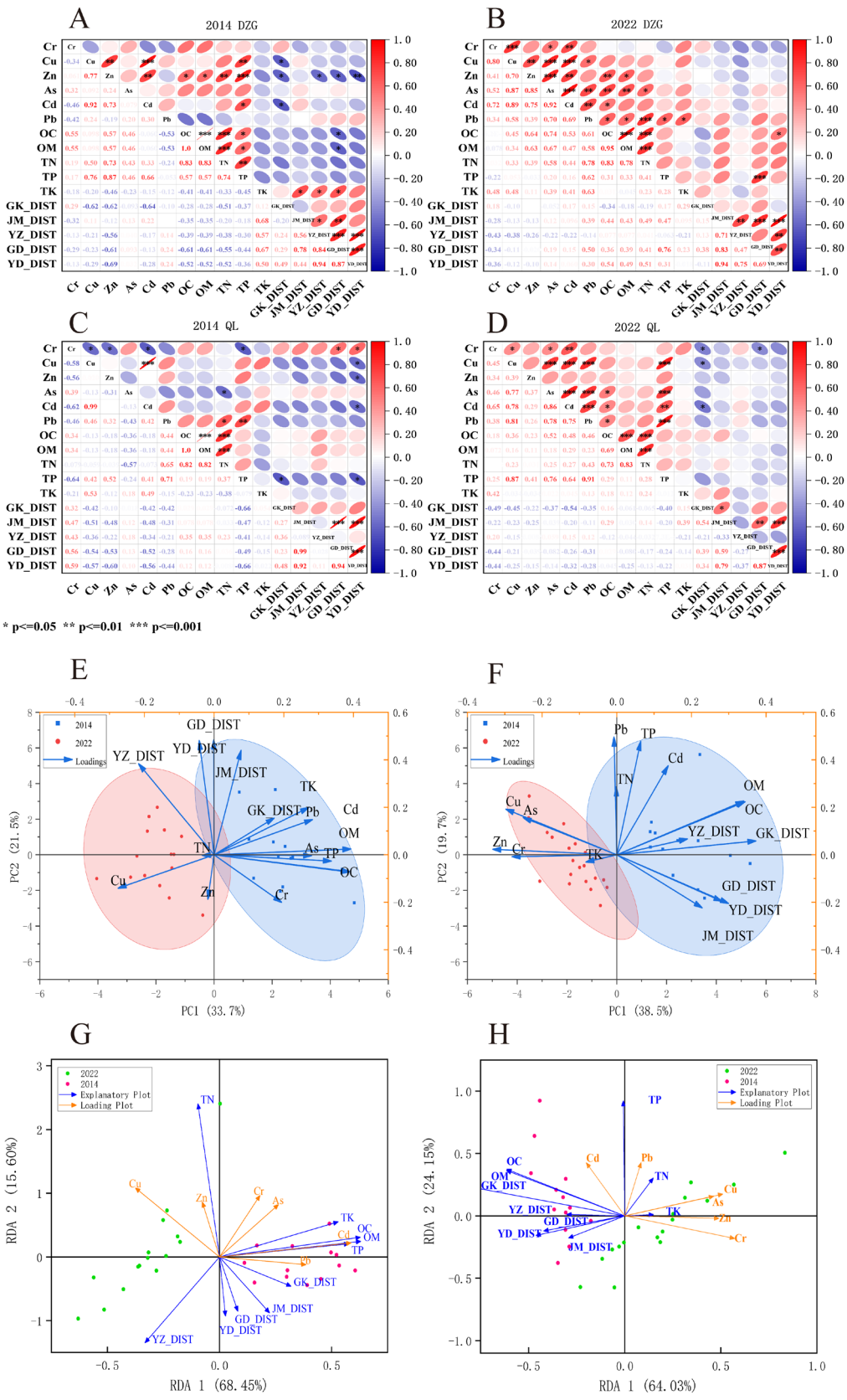

Figure 5. Statistical analysis between heavy metals in sediments and environmental factors. (**A**,**B**) show correlation analysis between heavy metals in sediments and environmental factors in DZG in 2014 and 2022. (**C**,**D**) show correlation analysis between heavy metals in sediments and environmental factors in QL in 2014 and 2022. (**E**,**F**) show principal component analysis of DZG and QL. (**G**,**H**) show redundancy analysis of the study area DZG and QL.

In QL, RDA1 accounted for 64.03% of the variation, and RDA2 accounted for 24.15% of the variation. Figure 5H shows overlap and differences in data point distribution on both axes between 2014 and 2022. In 2014, QL was mainly influenced by OC, OM, and GK_DIST, indicating that sediment heavy metals were related to soil fertility or organic pollution. In 2022, TP, OC, OM, and GK_DIST had significant impacts on QL. Cr, Cu, As, and Zn showed strong positive correlations with TN and TP, indicating that these heavy metals were influenced by nutrient salts and changes in land use types. Cd and Pb were negatively correlated with distances to industrial and mining enterprises and residential areas. From 2014 to 2022, the heavy metal contents in QL changed significantly, with notable increases in Cr and As that were likely due to increased industrial and agricultural activities and rapid urbanization in the surrounding area.

The degree of data point separation on the RDA plot reflects the magnitude of environmental changes during the study period. After comparing data from 2014 and 2022, DZG's data separation was more pronounced than QL's, indicating that more significant environmental changes had occurred in DZG. Combined with previous analyses, it can be concluded that DZG's environment is superior to QL's. This finding also demonstrates that protecting and maintaining the environment around mangroves and reasonably managing human activities in these areas are crucial for producing a reduction in heavy metal contents in sediments in these areas.

4.2.2. Analysis of Heavy Metal Fate

Table 1 and Figures 2 and 3 demonstrate that the concentrations of most heavy metals in the sediments of DZG and QL showed a downward trend over the past decade. Generally, in addition to anthropogenic engineering and physicochemical treatments that can lead to reductions in heavy metal concentrations, bioremediation and agricultural management are also important measures for producing a decline in heavy metal contents. Mangrove plants play a significant role in the absorption and translocation of heavy metals in coastal ecosystems [43]. Through a series of complex physiological mechanisms that include avoidance, chelation, compartmentalization, tolerance, secretion, and filtration, they effectively mitigate the pollution impacts of heavy metals [5]. Agricultural management involves adapting land use practices and management systems to produce reductions in heavy metal hazards on utilized lands or the transport of heavy metals to downstream areas. To date, no anthropogenic engineering or physicochemical methods have been applied to remediate heavy metal pollution in the mangrove sediments of the study area.

According to statistics from the DZG Management Authority, between 2013 and 2023, 385.07 ha of aquaculture ponds were removed within the DZG and its surrounding 5 km radius, and 301.53 ha of mangrove forests were restored. The mangrove area increased from 1578 to 1771.08 ha. Figure 4A shows that from 2015 to 2023, the mangrove land area within a 5 km radius of DZG increased by 319 ha, of which 222 ha came from the pond-to-mangrove conversion project. In QL and its surrounding areas, the net increase in mangrove area was 154 ha and was obtained mainly from non-mangrove forest land and aquaculture ponds. Clearly, the expansion of mangrove areas in the protected zones and their surroundings has enhanced the capacity of mangrove plants to absorb and translocate heavy metals, thus producing a certain "dilution effect".

5. Conclusions

(1) The mangrove sediments in DZG and QL generally exhibited low heavy metal concentrations, complying with China's Class I ecological–environmental quality standards. However, significant spatiotemporal heterogeneity was observed. Over the past decade, the Cd levels in both regions have declined markedly (greater than 40%), whereas the

Cr content in QL occasionally exceeded the Class I standard. Conversely, certain metals (e.g., Cu and Zn) show increasing trends, indicating persistent anthropogenic inputs. Spatially, heavy metal distribution is governed by a combination of geographic, anthropogenic, and ecological factors, displaying distinct heterogeneity. Elevated concentrations were found in DZG's southeast (driven by industrial/aquaculture activities) and QL's northwest (influenced by urban/industrial discharges), underscoring land–sea–human interactions as key drivers. In DZG, the weakening correlations between Cd, Cr, and environmental factors (e.g., industrial proximity and TP) suggest reduced human impact, likely due to mangrove restoration (319 ha expansion, including 222 ha converted from aquaculture ponds), which enhanced metal sequestration and dilution. In QL, the levels were found to be relatively lower in the south but higher in the northwest and northeast, where Cr's strong negative correlation with industrial distance confirms ongoing pollution from mining and urbanization. These patterns highlight the dominant role of anthropogenic activities in reshaping mangrove sediment environments.

(2) Overall, the ecological status of the two nature reserves is good, with low ecological risk. However, the Cd concentration in QL has reached a moderate risk level, highlighting the urgency of industrial pollution control. A collaborative governance system integrating "land-based interception and mangrove filtration" should be established. Efforts should be intensified to improve water quality in the areas surrounding QL, with strict control over the discharge of industrial, urban, and aquaculture wastewater to mitigate the potential threats of heavy metals to mangrove ecosystems.

(3) Beyond natural influences from rock weathering, heavy metals in DZG were initially affected by industrial, mining, agricultural, and aquaculture practices, but their impact has diminished over time, as evidenced by declining correlations with human-related factors and stronger inter-metal associations. In contrast, QL's heavy metal distribution remains heavily influenced by human activities, particularly industrial expansion and nutrient inputs. RDA analysis indicates strong negative correlations between Cr and environmental factors such as distance to industrial areas, OC, TP, and orchard land, highlighting the significant impact of these factors on heavy metal distribution. Pond-to-mangrove conversion projects implemented in and around the two reserves exhibited a "dilution effect" on heavy metal content in sediments. Mangroves represent a natural and sustainable solution to heavy metal pollution in coastal areas. This finding underscores the potential of mangroves in heavy metal pollution remediation and provides valuable theoretical and practical guidance for future ecological restoration efforts.

Author Contributions: Conceptualization, T.S. and P.Q.; methodology, T.S.; software, T.S. and W.Z.; formal analysis, T.S.; investigation, T.S., Q.S., W.Z. and M.J.; resources, C.C.; writing—original draft preparation, T.S.; review and editing, T.S., P.Q. and L.L.; visualization, T.S.; funding acquisition, P.Q. and Y.Y. All authors have read and agreed to the published version of the manuscript.

Funding: This research was funded by the National Natural Science Foundation of China (grant numbers 42061048, 32101525, and 42401071); the Innovation Platform for Academicians of Hainan Province and its specific research fund (grant number YSPTZX202128); and the Hainan Provincial Natural Science Foundation of China (grant numbers 425RC756, 421QN236 and 224MS057).

Data Availability Statement: The raw data will be made available upon request from the corresponding author.

Conflicts of Interest: Author Chuanzhao Chen is employed by Hainan Guoyuan Land and Mineral Survey Planning & Design Co., Ltd. (a technical service enterprise under Hainan Provincial Engineering Consulting & Design Group). The company provides non-profit technical support to government natural resource management projects. No commercial benefits were derived from this research. Other authors declare no conflicts of interest.

Appendix A

Table A1. Changes in major land use types in the catchment areas of the study area (km^2).

Land Use Type	DZG			QL		
	2014	2022	Change	2014	2022	Change
Arable land	307.18	285.09	−22.10	215.95	173.78	−42.18
Orchard land	167.15	157.52	−9.63	268.45	298.64	30.19
Forest land	202.79	218.78	15.99	224.68	255.50	30.82
Aquaculture ponds	46.58	46.95	0.37	53.03	57.31	4.28
Facility agricultural land	5.46	7.30	1.84	2.43	5.88	3.45
Urban land	13.43	21.78	8.34	21.47	29.68	8.21
Industrial and mining land	1.32	4.34	3.02	1.09	5.46	4.37
Transportation land	5.70	14.59	8.90	3.56	23.56	20.00

Appendix B

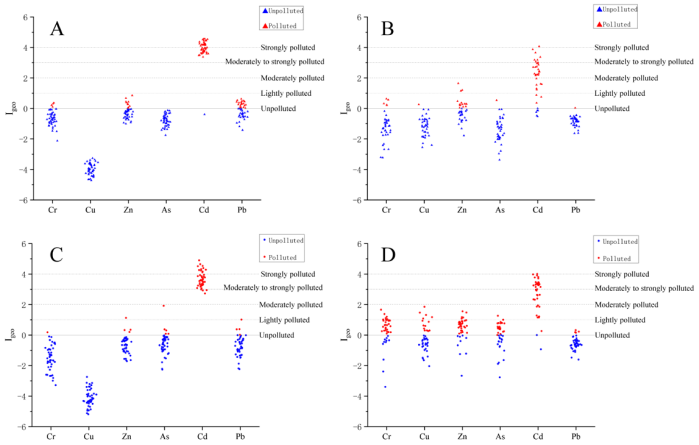

Figure A1. Comparison of geo-accumulation index of sediments from study areas in different years. (**A**) shows DZG in 2014. (**B**) shows DZG in 2022. (**C**) shows QL in 2014. (**D**) shows QL in 2022.

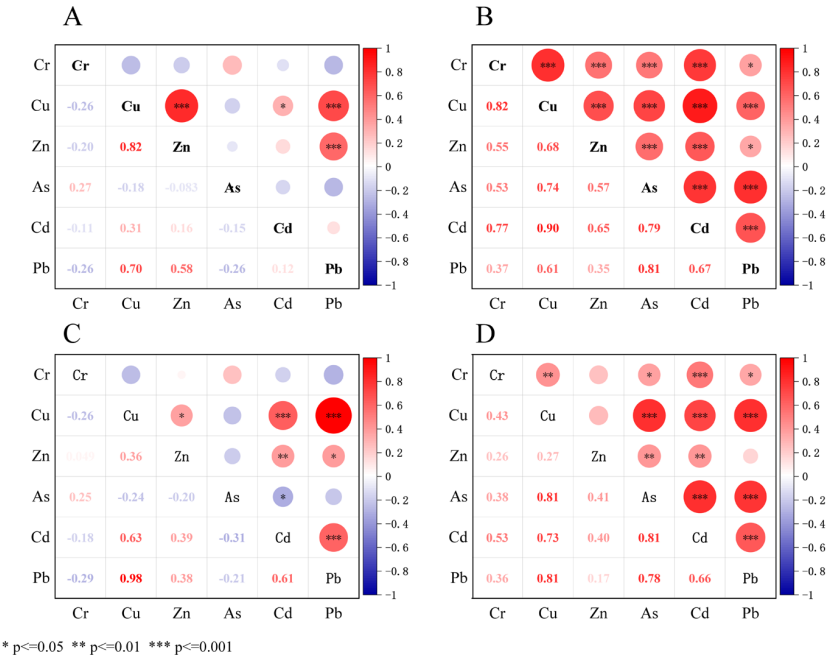

Figure A2. Correlations analysis of heavy metal contents in mangrove sediments in the study area. (**A**) shows DZG in 2014. (**B**) shows DZG in 2022. (**C**) shows QL in 2014. (**D**) shows QL in 2022.

References

1. Kumar, S.; Akash, P.B.; Islam, R.; MacFarlane, G.R. Pollution Status and Ecological Risk Assessment of Metal(Loid)s in the Sediments of the World's Largest Mangrove Forest: A Data Synthesis in the Sundarbans. *Mar. Pollut. Bull.* **2023**, *187*, 114514. [CrossRef]
2. Dutta Roy, A.; Pitumpe Arachchige, P.S.; Watt, M.S.; Kale, A.; Davies, M.; Heng, J.E.; Daneil, R.; Galgamuwa, G.A.P.; Moussa, L.G.; Timsina, K.; et al. Remote Sensing-Based Mangrove Blue Carbon Assessment in the Asia-Pacific: A Systematic Review. *Sci. Total Environ.* **2024**, *938*, 173270. [CrossRef]
3. Zhang, G.; Chen, S.; Long, R.; Ma, B.; Chang, Y.; Mao, C. Distribution of Heavy Metals in Surface Sediments of a Tropical Mangrove Wetlands in Hainan, China, and Their Biological Effectiveness. *Minerals* **2023**, *13*, 1476. [CrossRef]
4. Ma, Y.; Wang, W.; Gao, F.; Yu, C.; Feng, Y.; Gao, L.; Zhou, J.; Shi, H.; Liu, C.; Kong, D.; et al. Acidification and Hypoxia in Seawater, and Pollutant Enrichment in the Sediments of Qi'ao Island Mangrove Wetlands, Pearl River Estuary, China. *Ecol. Indic.* **2024**, *158*, 111589. [CrossRef]
5. Ur Rahman, S.; Han, J.-C.; Zhou, Y.; Ahmad, M.; Li, B.; Wang, Y.; Huang, Y.; Yasin, G.; Ansari, M.J.; Saeed, M.; et al. Adaptation and Remediation Strategies of Mangroves against Heavy Metal Contamination in Global Coastal Ecosystems: A Review. *J. Clean. Prod.* **2024**, *441*, 140868. [CrossRef]
6. Deng, J.; Guo, P.; Zhang, X.; Shen, X.; Su, H.; Zhang, Y.; Wu, Y.; Xu, C. An Evaluation on the Bioavailability of Heavy Metals in the Sediments from a Restored Mangrove Forest in the Jinjiang Estuary, Fujian, China. *Ecotoxicol. Environ. Saf.* **2019**, *180*, 501–508. [CrossRef]
7. Hu, C.; Ma, Y.; Liu, Y.; Wang, J.; Li, B.; Sun, Y.; Shui, B. Trophodynamics and Potential Health Risk Assessment of Heavy Metals in the Mangrove Food Web in Yanpu Bay, China. *Sci. Total Environ.* **2024**, *920*, 171028. [CrossRef]
8. Elumalai, P.; Parthipan, P.; Gao, X.; Cui, J.; Kumar, A.S.; Dhandapani, P.; Rajasekar, A.; Sarma, H.; Ganapathy, N.R.V.; Theerthagiri, J.; et al. Impact of Petroleum Hydrocarbon and Heavy Metal Pollution on Coral Reefs and Mangroves: A Review. *Environ. Chem. Lett.* **2024**, *22*, 1413–1435. [CrossRef]
9. Ouyang, X.; Guo, F.; Lee, S.Y.; Yang, Z. Mangrove Restoration in China's Tidal Ecosystems. *Science* **2024**, *385*, 836. [CrossRef]
10. Wang, Z.; Liu, K.; Cao, J.; Peng, L.; Wen, X. Annual Change Analysis of Mangrove Forests in China during 1986–2021 Based on Google Earth Engine. *Forests* **2022**, *13*, 1489. [CrossRef]
11. Zhu, Y.; Jia, P.; Zhang, Z.; Cheng, J.; Wang, N. Carbon Storage Assessment under Mangrove Restoration of Dongzhai Harbor in Hainan Island, China. *Ecosyst. Health Sustain.* **2024**, *10*, 257. [CrossRef]
12. Fang, F.Z.; Li, Z.J.; Gui, H.Y. Investigation and Research on the Current Situation of Mangrove Forest in Hainan. *Trop. For.* **2022**, *50*, 42–49. (In Chinese)
13. Hu, C.; Liu, Y.; Fang, X.; Zhou, Z.; Yu, Y.; Sun, Y.; Shui, B. Assessing Heavy Metal Pollution in Sediments from the Northern Margin of Chinese Mangrove Areas: Sources, Ecological Risks, and Health Impacts. *Mar. Pollut. Bull.* **2024**, *200*, 116069. [CrossRef]
14. Zhao, Y.Y.; Yan, M.C. Chemical Element Abundance of Shallow Sea Sediments in China. *Sci. China Ser. B Chem. Life Sci. Geosci.* **1993**, 1084–1090. (In Chinese)
15. Hakanson, L. An Ecological Risk Index for Aquatic Pollution Control.a Sedimentological Approach. *Water Res.* **1980**, *14*, 975–1001. [CrossRef]
16. Wang, C.; He, S.; Zou, Y.; Liu, J.; Zhao, R.; Yin, X.; Zhang, H.; Li, Y. Quantitative Evaluation of In-Situ Bioremediation of Compound Pollution of Oil and Heavy Metal in Sediments from the Bohai Sea, China. *Mar. Pollut. Bull.* **2020**, *150*, 110787. [CrossRef] [PubMed]
17. Yi, Y.; Yang, Z.; Zhang, S. Ecological Risk Assessment of Heavy Metals in Sediment and Human Health Risk Assessment of Heavy Metals in Fishes in the Middle and Lower Reaches of the Yangtze River Basin. *Environ. Pollut.* **2011**, *159*, 2575–2585. [CrossRef]
18. *HJ 1300-2023*; Technical Specification for Quality Assessment of Seawater, Marine Sediments and Marine Organisms. Ministry of Ecology and Environment of the People's Republic of China: Beijing, China, 2023.
19. Xu, X.R.; Xie, G.Z.; Qiu, P.H. Dynamic Analysis of Landscape Changes in Bamen Port and the Surrounding Lands of Hainan Province from 1964 to 2015. *Acta Ecol. Sin.* **2018**, *38*, 7458–7468. (In Chinese) [CrossRef]
20. Li, R.; Li, R.; Chai, M.; Shen, X.; Xu, H.; Qiu, G. Heavy Metal Contamination and Ecological Risk in Futian Mangrove Forest Sediment in Shenzhen Bay, South China. *Mar. Pollut. Bull.* **2015**, *101*, 448–456. [CrossRef]
21. Wu, Q.; Tam, N.F.Y.; Leung, J.Y.S.; Zhou, X.; Fu, J.; Yao, B.; Huang, X.; Xia, L. Ecological Risk and Pollution History of Heavy Metals in Nansha Mangrove, South China. *Ecotoxicol. Environ. Saf.* **2014**, *104*, 143–151. [CrossRef]
22. Geng, J.J.; Huang, L.L.; Wu, Z.Q.; Zhu, Z.J.; Chang, T.; Wu, W.L.; Xiong, L. Accumulation Characteristics of Heavy Metals in Mangrove Wetland Plants in Maowei Sea. *J. Guilin Univ. Technol.* **2015**, *35*, 138–141. (In Chinese)
23. Xie, Z.; Zhu, G.; Xu, M.; Zhang, H.; Yi, W.; Jiang, Y.; Liang, M.; Wang, Z. Risk Assessment of Heavy Metals in a Typical Mangrove Ecosystem—A Case Study of Shankou Mangrove National Natural Reserve, Southern China. *Mar. Pollut. Bull.* **2022**, *178*, 113642. [CrossRef] [PubMed]

24. Mackey, A.P.; Hodgkinson, M.C. Concentrations and Spatial Distribution of Trace Metals in Mangrove Sediments from the Brisbane River, Australia. *Environ. Pollut.* **1995**, *90*, 181–186. [CrossRef] [PubMed]
25. Balakrishnan, B.; Sahu, B.K.; Kothilmozhian Ranishree, J.; Lourduraj, A.V.; Nithyanandam, M.; Packiriswamy, N.; Panchatcharam, P. Assessment of Heavy Metal Concentrations and Associated Resistant Bacterial Communities in Bulk and Rhizosphere Soil of Avicennia Marina of Pichavaram Mangrove, India. *Environ. Earth Sci.* **2017**, *76*, 58. [CrossRef]
26. Ramanathan, A.L.; Subramanian, V.; Ramesh, R.; Chidambaram, S.; James, A. Environmental Geochemistry of the Pichavaram Mangrove Ecosystem (Tropical), Southeast Coast of India. *Environ. Geol.* **1999**, *37*, 223–233. [CrossRef]
27. Jonathan, M.P.; Sarkar, S.K.; Roy, P.D.; Alam, M.A.; Chatterjee, M.; Bhattacharya, B.D.; Bhattacharya, A.; Satpathy, K.K. Acid Leachable Trace Metals in Sediment Cores from Sunderban Mangrove Wetland, India: An Approach towards Regular Monitoring. *Ecotoxicology* **2010**, *19*, 405–418. [CrossRef]
28. Fernández-Cadena, J.C.; Andrade, S.; Silva-Coello, C.L.; De la Iglesia, R. Heavy Metal Concentration in Mangrove Surface Sediments from the North-West Coast of South America. *Mar. Pollut. Bull.* **2014**, *82*, 221–226. [CrossRef]
29. Hasan, M.R.; Anisuzzaman, M.; Choudhury, T.R.; Arai, T.; Yu, J.; Albeshr, M.F.; Hossain, M.B. Vertical Distribution, Contamination Status and Ecological Risk Assessment of Heavy Metals in Core Sediments from a Mangrove-Dominated Tropical River. *Mar. Pollut. Bull.* **2023**, *189*, 114804. [CrossRef]
30. Page, A.L.; Bingham, F.T. Cadmium residues in the environment. In *Residue Reviews*; Gunther, F.A., Gunther, J.D., Eds.; Springer: New York, NY, USA, 1973; Volume 48. [CrossRef]
31. Qiu, P.H.; Wang, D.Z.; Xie, G.Z.; Xu, S.J.; Cao, R.; Wang, J.G. Comparison of Heavy Metal Pollution, Enrichment, and Transport Capacity Between Artificial and Natural Mangroves in Hainan Island. *Trop. Geogr.* **2018**, *38*, 836–847. (In Chinese) [CrossRef]
32. Tang, D.; Luo, S.; Deng, S.; Huang, R.; Chen, B.; Deng, Z. Heavy Metal Pollution Status and Deposition History of Mangrove Sediments in Zhanjiang Bay, China. *Front. Mar. Sci.* **2022**, *9*, 989584. [CrossRef]
33. Yang, Q.; Shen, X.; Jiang, H.; Luan, T.; Yang, Q.; Yang, L. Key Factors Influencing Pollution of Heavy Metals and Phenolic Compounds in Mangrove Sediments, South China. *Mar. Pollut. Bull.* **2023**, *194*, 115283. [CrossRef] [PubMed]
34. Liu, J.; Myat, T. Contaminants and Heavy Metals Along the Mangrove Area of Dongzhai Harbor, China: Distribution and Assessment. *SN Appl. Sci.* **2021**, *3*, 823. [CrossRef]
35. Wang, H.; Wang, J.; Liu, R.; Yu, W.; Shen, Z. Spatial variation, environmental risk and biological hazard assessment of heavy metals in surface sediments of the Yangtze river estuary. *Mar. Pollut. Bull.* **2015**, *93*, 250–258. [CrossRef]
36. Zheng, R.; Liu, Y.; Zhang, Z. Trophic Transfer of Heavy Metals through Aquatic Food Web in the Largest Mangrove Reserve of China. *Sci. Total Environ.* **2023**, *899*, 165655. [CrossRef]
37. Pang, G.T.; Yang, Y.Z.; Luo, J.S.; Qu, Z.S.; Liu, K.K.; Qiao, Y.; Yu, S.H.; Ni, H.J. Distribution Characteristics and Ecological Risk Assessment of Heavy Metals in Sediments of Mangrove Wetlands in Fangchenggang. *J. Guangdong Ocean Univ.* **2024**, *44*, 69–75. (In Chinese)
38. Huang, Z.Y.; Guan, D.S.; Wang, G. Impact of Socio-Economic Development on Heavy Metal Pollution in Surface Soils of Mangroves in Hainan Island. *Mar. Environ. Sci.* **2020**, *39*, 831–837. (In Chinese) [CrossRef]
39. Fu, K.; Chen, Z.; Huang, C.; Chen, Y.; Wu, D.; Li, X.; Song, Y.; Ding, W.; Yang, X.; Long, J. Distribution, Sources, Impact Factors and Ecological Risks of Sediment Heavy Metals from Typical Estuarine Wetlands in Tropical Islands. *Estuar. Coast. Shelf Sci.* **2024**, *307*, 108922. [CrossRef]
40. Cao, R.; Qiu, P.H.; Xie, G.Z. Water Quality Analysis of Dongzhai Harbor Mangrove Based on Fuzzy Evaluation and Buffer Gradient Zone. *Water Sav. Irrig.* **2017**, 58–63+68. (In Chinese)
41. Liu, J.; Wu, H.; Feng, J.; Li, Z.; Lin, G. Heavy Metal Contamination and Ecological Risk Assessments in the Sediments and Zoobenthos of Selected Mangrove Ecosystems, South China. *Catena* **2014**, *119*, 136–142. [CrossRef]
42. Superville, P.-J.; Prygiel, E.; Magnier, A.; Lesven, L.; Gao, Y.; Baeyens, W.; Ouddane, B.; Dumoulin, D.; Billon, G. Daily Variations of Zn and Pb Concentrations in the Deûle River in Relation to the Resuspension of Heavily Polluted Sediments. *Sci. Total Environ.* **2014**, *470–471*, 600–607. [CrossRef]
43. Yadav, K.K.; Gupta, N.; Prasad, S.; Malav, L.C.; Bhutto, J.K.; Ahmad, A.; Gacem, A.; Jeon, B.-H.; Fallatah, A.M.; Asghar, B.H.; et al. An Eco-Sustainable Approach Towards Heavy Metals Remediation by Mangroves from the Coastal Environment: A Critical Review. *Mar. Pollut. Bull.* **2023**, *188*, 114569. [CrossRef] [PubMed]